Plasmaspheric mass loss and refilling as a result of a magnetic storm

B. W. Reinisch,[1] X. Huang,[1] P. Song,[1] J. L. Green,[2] S. F. Fung,[2] V. M. Vasyliunas,[3] D. L. Gallagher,[4] and B. R. Sandel[5]

Received 20 March 2003; revised 4 August 2003; accepted 28 August 2003; published 6 January 2004.

[1] Using the sounding measurements from the radio plasma imager on IMAGE and a plasma density inversion algorithm, we derive the plasma density profiles along the magnetic field in a few L shells every 14 hours at magnetic local noon before, during, and after the 31 March 2001 magnetic storm. An empirical model of the plasmaspheric plasma density distribution is derived as a reference using the measurements before the storm. During the storm the equatorial plasma was substantially depleted in a range of L shells. The flux tubes were refilled after the storm. The filling ratio, the equatorial plasma density normalized by its quiet time value before the storm, is introduced to assess the time evolution of the depletion and refilling processes. The depletion, more than two thirds of the quiet time content, appeared to occur rather quickly after the storm onset, as determined by the limited temporal resolution of the measurements. The refilling proceeded, although more slowly than the depletion process, significantly faster than the theoretical prediction of a 3-day timescale. Dynamic structures are observed in situ and confirmed by the extreme ultraviolet imager (EUV) measurements. *INDEX TERMS:* 2768 Magnetospheric Physics: Plasmasphere; 2788 Magnetospheric Physics: Storms and substorms; 2730 Magnetospheric Physics: Magnetosphere—inner; 2740 Magnetospheric Physics: Magnetospheric configuration and dynamics; *KEYWORDS:* plasmasphere, magnetic storm, plasmasphere refilling, plasmasphere depletion, plasmasphere model

Citation: Reinisch, B. W., X. Huang, P. Song, J. L. Green, S. F. Fung, V. M. Vasyliunas, D. L. Gallagher, and B. R. Sandel (2004), Plasmaspheric mass loss and refilling as a result of a magnetic storm, *J. Geophys. Res.*, *109*, A01202, doi:10.1029/2003JA009948.

1. Introduction

[2] In addition to the processes that determine the nature and variation of the sources of magnetospheric plasma in the ionosphere, magnetospheric dynamic processes and global convection determine the plasma distribution and redistribution. Part of the plasmaspheric plasma can be depleted and later refilled during magnetic storms. Corotating structures, such as shoulders, fingers, notches, channels, and plasma plumes [e.g., *Grebowsky*, 1970; *Chen et al.*, 1975; *Sandel et al.*, 2001; *Burch et al.*, 2001a; *Goldstein et al.*, 2003; *Carpenter et al.*, 2002] can be formed. Since the magnetospheric plasma density distribution may be controlled by the loss-refilling and other dynamic processes, it may vary substantially according to its stage relative to a storm/substorm onset. Therefore an instantaneous measurement of the plasma density along the field line is critical to the understanding of the dynamic processes that determine the distribution of the plasma along a flux tube.

[3] The plasma density distribution along the magnetic field has long attracted much interest because it is a test bed for various theoretical models involving different physical processes. The main source of the plasma is the ionosphere. The ionization rate in the ionosphere depends strongly on latitude, local time, seasonal effects, and the magnetospheric precipitations. A steady state plasmaspheric density distribution can be reached when the filling rate balances the loss rate to the magnetosphere or solar wind. In the past, direct measurements of field-aligned plasma distribution were nearly impossible except by using statistical analyses [e.g., *Persoon et al.*, 1983; *Horwitz et al.*, 1990; *Carpenter and Anderson*, 1992; *Gallagher et al.*, 2000; *Goldstein et al.*, 2001; *Denton et al.*, 2001]. During dynamic magnetospheric events, such as magnetic storms, the plasma distribution may vary substantially both in space and time, compromising the value of statistical models. Extensive investigations combining in situ measurements and numerical models have also been carried out. One such effort is the combination of the field line interhemispheric plasma (FLIP) model [*Richards et al.*, 1983] with the Dynamic Explorer (DE) in situ observations [*Newberry et al.*, 1989;

[1]Environmental, Earth, and Atmospheric Sciences Department, Center for Atmospheric Research, University of Massachusetts Lowell, Lowell, Massachusetts, USA.
[2]NASA Goddard Space Flight Center, Greenbelt, Maryland, USA.
[3]Max-Planck-Institut für Aeronomie, Katlenburg-Lindau, Germany.
[4]NASA Marshal Space Flight Center, Huntsville, Alabama, USA.
[5]Lunar and Planetary Laboratory, University of Arizona, Tucson, Arizona, USA.

0148-0227/04/2003JA009948$09.00

Horwitz et al., 1990; *Comfort et al.*, 1995]. These model simulations may describe the dynamic processes along the magnetic field, but have to be confirmed by observations covering large spatial scales. *Tu et al.* [2003] recently have initiated such an observation-simulation comparison.

[4] The depletion of the plasmaspheric particles during storms was first reported by *Carpenter* [1963], using ground-based whistler wave measurements, and later by *Horwitz et al.* [1984] using DE observations. These observations were made at each individual location, making the quantitative assessment of total depletion difficult, if not impossible. In this study, we use a new technique based on radio plasma imager (RPI) measurements on IMAGE [*Burch et al.*, 2001b] and a plasma density inversion algorithm to derive the plasma density along the magnetic field. With enough measurements at different L values, which are the equatorial geocentric distance of a dipole magnetic field line in Earth radii, during quiet times before a storm, a quiet time two-dimensional (2-D) plasma distribution along the IMAGE orbit can be obtained for the event. Plasma density profiles along the field at similar magnetic local times were obtained on every IMAGE orbit during and after the storm so that the depletion and refilling processes could be assessed from a common reference level in the equatorial plane.

2. Sounding Measurements and the Plasma Density Inversion Technique

[5] RPI [*Reinisch et al.*, 2000] on IMAGE, in its active experiment, transmits coded signals into all directions, scanning through the frequency band from nominally 3 kHz to 3 MHz. At each frequency, after transmission of a 3.3 ms pulse, the RPI waits for echoes that are reflected back to the satellite, and the echo delay times are recorded. Echoes in the "plasmagram," a display of signal amplitude as functions of frequency and echo delay time as shown in Figure 1 (top), often form traces. In Figure 1 (top), the color coding shows the signal amplitudes, the vertical axis is time delay multiplied by $c/2$, and presented as the so-called virtual range (here given in Earth radii R_E), and the horizontal axis is frequency in kHz. Each complete measurement of this type was made in less than 2 min. For each frequency, the measurement was made in a fraction of a second. Generating an echo requires the existence of a reflection point at which the index of refraction of a mode is zero and the incident signal is parallel to the gradient of the refraction index. These two conditions reduce the reflection points to limited regions in space, however they specify the plasma conditions at each reflection point. The echo signal frequency is positively correlated with the plasma density at the reflection point, a known theoretical relationship. By measuring the time delays of all the echoes in an echo trace, the distances to the reflection points can be determined if the exact paths along which the signals traveled are known.

[6] An echo trace is formed from echoes that experience the same dispersion in the propagation. The fact that only a limited number of traces are observed implies that only few possible propagation directions and paths produce echoes. With extensive numerical simulations [*Reinisch et al.*, 2001a, 2001b], it appears that strong discrete traces are often formed by X mode propagations nearly along the magnetic field. Only two discrete traces are seen in Figure 1 (top), one corresponding to waves arriving parallel, the other to waves arriving antiparallel to the field.

[7] The plasmagrams generally also show vertical lines of enhanced signals. They occur at local plasma characteristic frequencies produced by local plasma emissions stimulated by the RPI transmissions [*Benson et al.*, 2003, and references therein]. Most frequently, they occur at the local plasma frequency, the upper hybrid frequency, and the harmonics of the electron gyrofrequency. For the case shown in Figure 1 (top), the local electron gyrofrequency predicted by the empirical magnetic field model [*Tsyganenko and Stern*, 1996] at the start time of the plasmagram is 36.5 kHz. The short vertical trace at 150 kHz is attributed to the fourth gyrofrequency harmonic, translating to an observed gyrofrequency of 37.5 kHz. The plasma frequency that gives an X mode cutoff frequency consistent with the observed start frequency of the x trace 238 kHz is 218 kHz and the upper hybrid frequency is 221 kHz, in agreement with observed vertical lines of enhanced signals on the plasmagram.

[8] From the two measured echo traces in Figure 1 (top), assuming propagation along the field line, the plasma density along the magnetic field for both hemispheres is derived, shown as the black line in Figure 1 (bottom), using a new profile inversion algorithm that is based on techniques used extensively in ionospheric sounding [*Huang and Reinisch*, 1982]. The plasmaspheric application of this method uses a model magnetospheric field [*Tsyganenko and Stern*, 1996]. The profile inversion algorithm has been carefully tested as described in an earlier report [*Reinisch et al.*, 2001b], which showed that the two strongest traces are indeed formed by X mode signals propagating nearly along the magnetic field. For the purpose of completeness it should be pointed out that the thin red lines in Figure 1 (top) are the simulated echo traces that are calculated for propagation along the field line and for the plasma density distribution given by the black line in Figure 1 (bottom). The dotted line portion of the density profile is interpolated based on the measured total electron content in this region and the assumption that the gradient of the plasma density is continuous.

3. Depleting and Refilling in the 31 March 2001 Storm

3.1. Quiet Time Plasma Density Distribution

[9] The measurements shown in Figure 1 (top) were made near local noon, at $L = 3.32$ at 2116 UT on 30 March 2001, before the 31 March storm, one of the biggest magnetic storms in solar cycle 23 with large geomagnetic perturbations and other accompanying phenomena. Figure 2 (top) shows the progress of the storm in *Dst*. The storm started near 0600 UT, 31 March 2001 (102 hours in the time plotted in Figure 2 that starts at 0000 UT on 27 March) and lasted for about 30 hours. The positions of the "spheres" in Figure 2 (bottom) show the L values and times when the measurements were made. Namely, for each sphere, there is a plasmagram of the type shown in Figure 1. The size of the spheres will be explained later. The IMAGE orbital period is about 14 hours. We take measurements only from the same region in each orbit, namely nearly at the same local noon and similar latitudes. Therefore the temporal resolution of our measurements in this study may be considered as

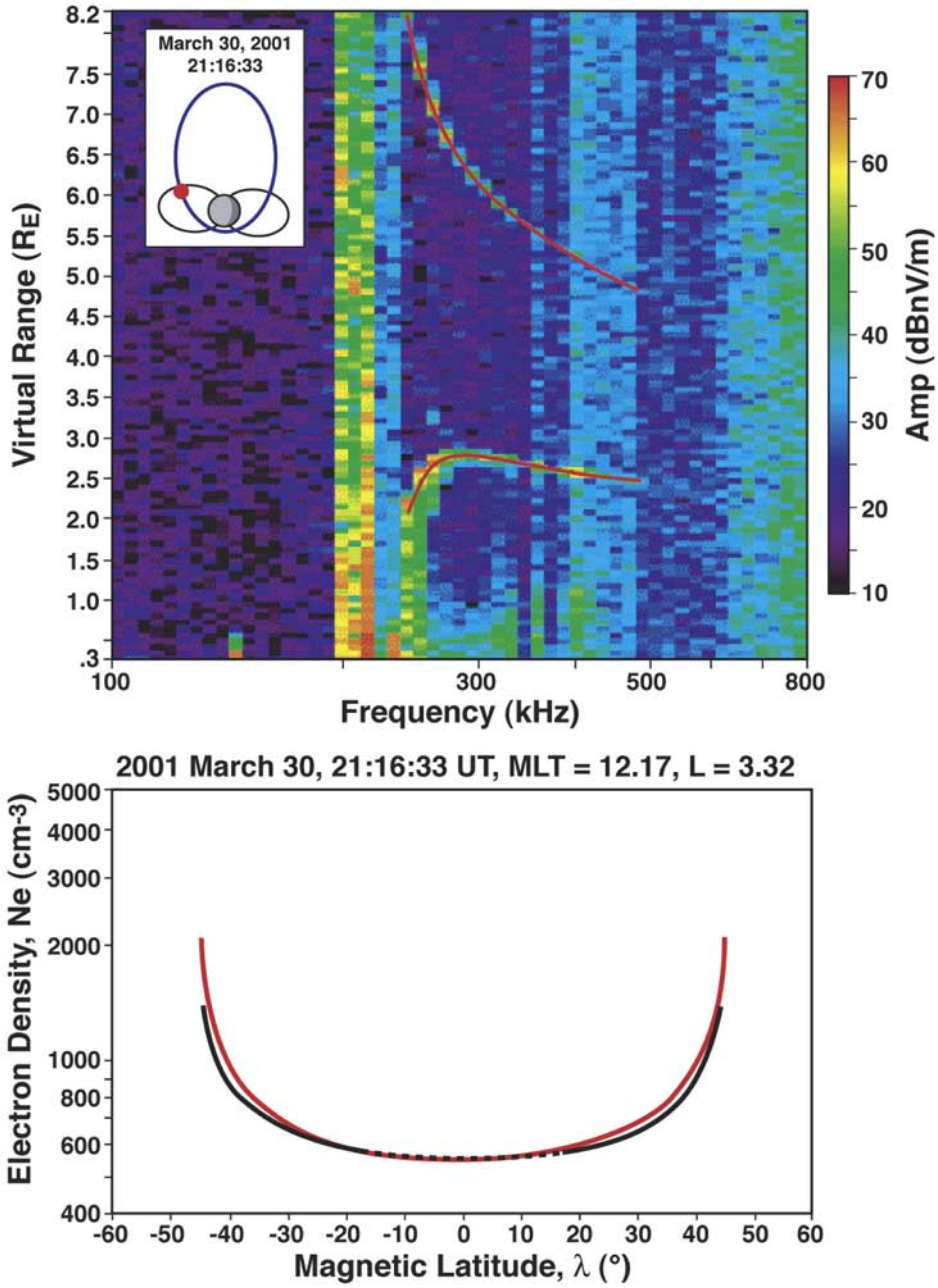

Figure 1. RPI measurements on 30 March 2001, before a storm event. (top) Plasmagram showing the echo amplitude as a function of frequency and virtual range in Earth radii (R_E). The rainbow color coding is proportion to the logarithm of the amplitude of the signals. The virtual range is the time delay of an echo multiplied by one half the free space speed of light c. Insert shows the orbit (blue), locations of IMAGE (red dot), and the L = 4 shells (black). (bottom) Plasma density profile along L = 3.32, black curve, as a function of magnetic latitude, derived from the measurements shown in Figure 1 (top). The red line in Figure 1 (bottom) is based on an empirical model that is discussed in connection with Figure 4. The red lines in the Figure 1 (top) are calculated echo traces based on the plasma densities shown by the black curve in Figure 1 (bottom). The electron gyrofrequency and the plasma frequency are 37.5 and 218 kHz, respectively.

14 hours although each individual profile determination corresponds to nearly instantaneous measurements and the series of measurements in each orbit covering a large range of L values were obtained within half an hour. There are data gaps in Figure 2 (bottom) around 2200 UT on 27 March, 1640 UT on 29 March, and 0640 UT on 30 March, because RPI was either operating at programs not suitable for our study or no identifiable trace was found. The reasons for missing identifiable traces and possible ducting propagation were discussed by *Reinisch et al.* [2001b]. Nine

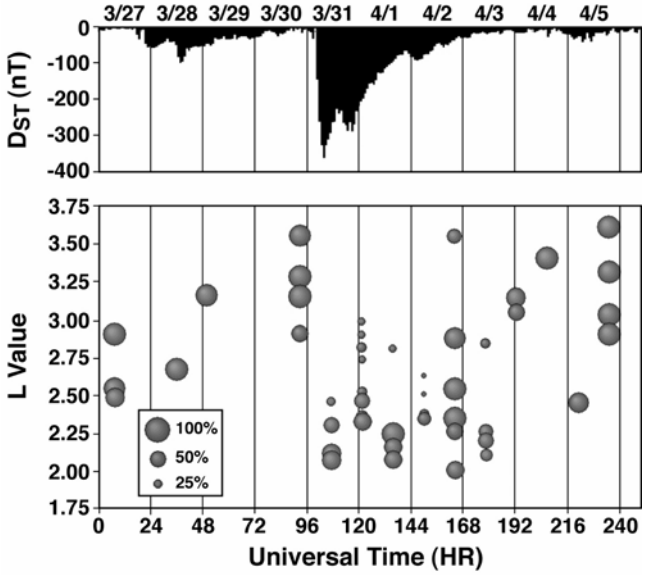

Figure 2. (top) Time history of the *Dst* index and (bottom) the filling ratio as function of L value and time. The size of the circles in Figure 2 (bottom) is proportional to the filling ratio. The filling ratio is defined as the measured equatorial density normalized by its quiet time value.

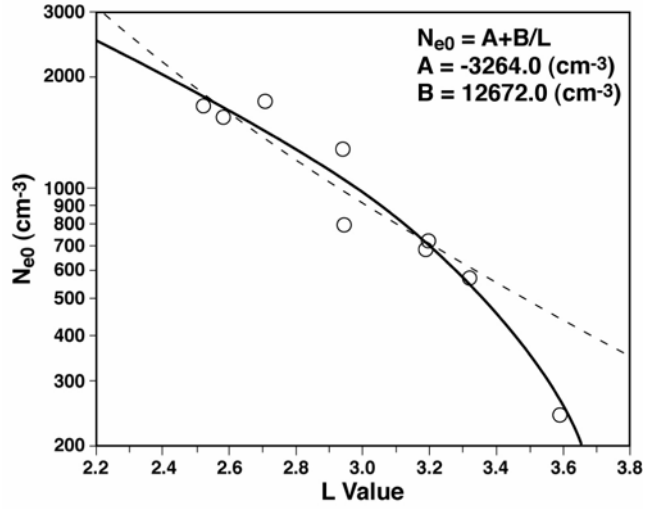

Figure 3. The equatorial plasma density as a function of L value from the measurements near 1200 MLT (open circles) before the storm event. The solid line shows the best fit hyperbolic function. The dashed line is the best fit L^{-4} function as predicted by the conservation of magnetic volume.

density profiles, however, were derived before the storm at various L values. Furthermore, in situ plasma frequency resonance measurements are used to confirm that each of the nine profiles is obtained in the plasmasphere. We will use the best fit of these measurements as the reference to assess the plasmasphere depletion and refilling. This reference is needed because each measurement during and after the storm was made at a particular L value and latitude, although at nearly the same magnetic local time, and we need to compare the values at a common plane, which is chosen as the equatorial plane.

[10] To derive an empirical model that describes the plasma density as a function of L and magnetic latitude λ, for the magnetic local time of the event, we first determine the functional form of the model because the dependence is highly nonlinear and because we want to minimize the number of fitting parameters in order to improve the robustness of our results. The measured plasma density profile shown in Figure 1 (bottom) (black curve), which is only a function of λ and not L, can be described by a minimum of three parameters (in the case of symmetry with regard to the magnetic equator): the equatorial plasma density value, the flatness of the bottom part of the profile at low and midlatitudes, and the steepness of the walls at higher latitudes. (The asymmetry seems unimportant in this case, although *Huang et al.* [2003] presented an expression for asymmetry about the equator.) After tests of various functional forms, we chose the following relation [*Song et al.*, 2003]:

$$N_e = N_{e0} \cos^{-\beta}\left(\frac{\pi}{2}\frac{\alpha\lambda}{\lambda_{inv}}\right) \quad (1)$$

where N_{e0}, α, and β specify the equatorial plasma density, the flatness, and the steepness, respectively, and λ_{inv} is the magnetic invariant latitude. In principle, the three parameters are functions of L. The L dependence of the profile flatness is explicitly given by λ_{inv}, making α only weakly dependent of L, and hence we assume α constant. On the basis of the best fit of nine profiles before the storm, the average α is 1.0, and the average β is 0.33. The equatorial plasma density N_{e0} decreases as L increases. Figure 3 shows N_{e0} as a function of L. We have explored various possible functions and found the best fit for an L^{-1} dependence giving $N_{e0}[\mathrm{cm}^{-3}] = 3264(3.88/L - 1)$, implying that the plasmapause was located within but near L = 3.88 where the

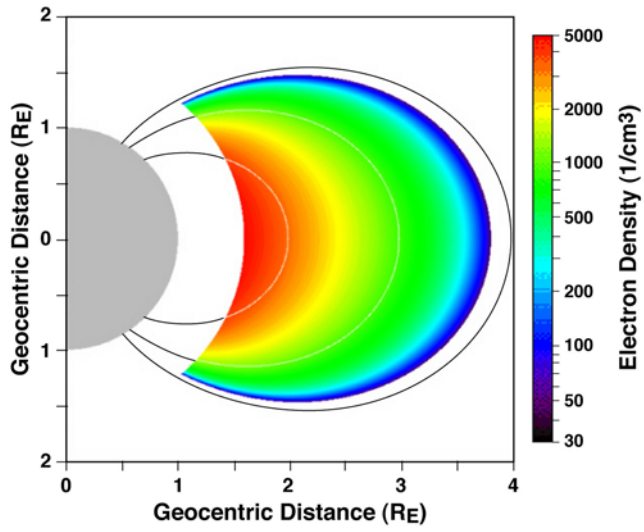

Figure 4. Two-dimensional color-coded plasma density distribution appropriate for 1200 MLT, derived from an empirical fit using the quiet time measurements before the storm.

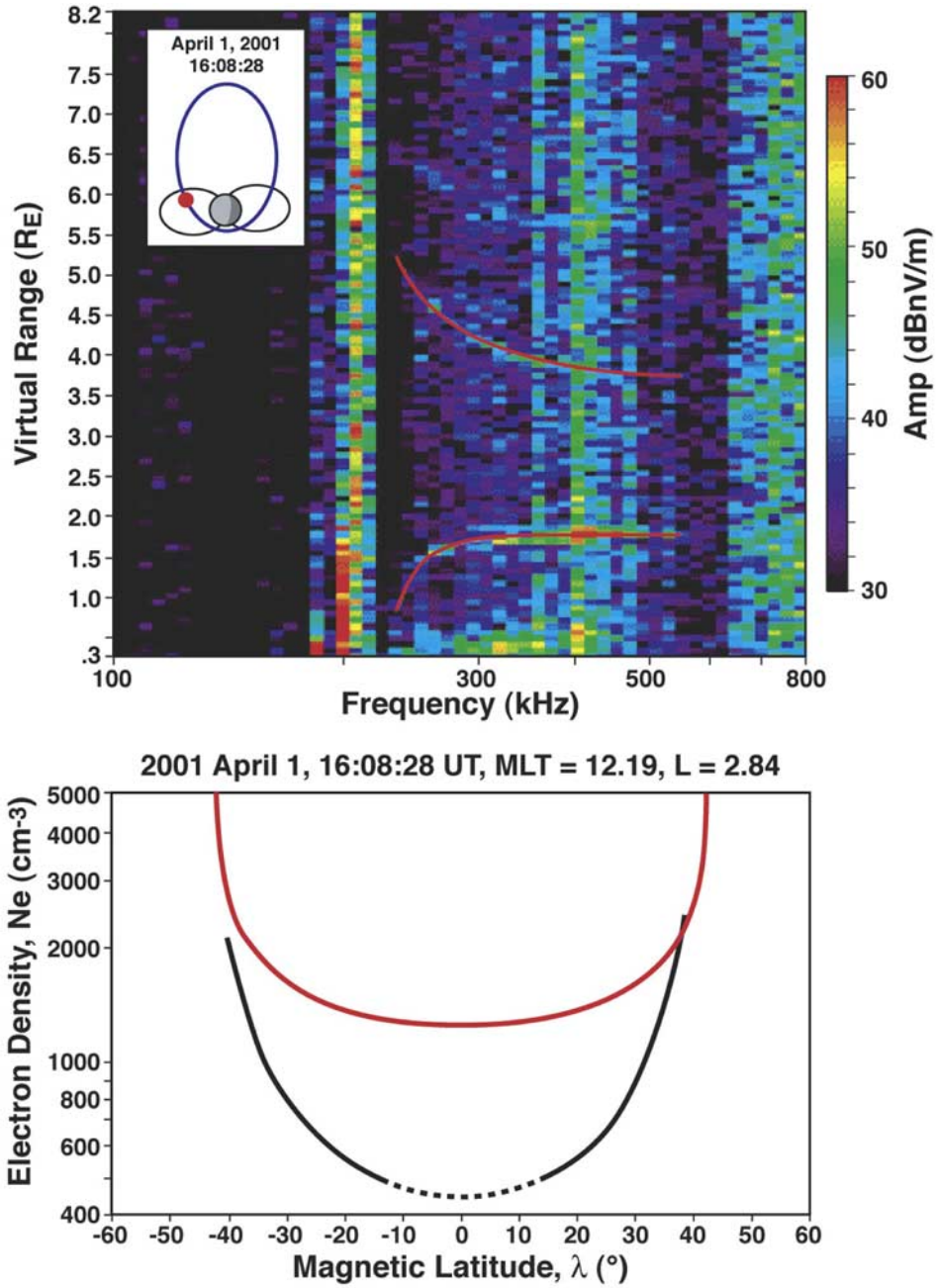

Figure 5. (top) RPI measurements and (bottom) the derived density profile in black during the storm event on 1 April 2001, for $L = 2.84$, in the same format as Figure 1. The red curve is the quiet time model profile. The electron gyrofrequency and the plasma frequency are 54.0 and 200 kHz, respectively.

model predicts the plasma density to be zero. This function is plotted as a solid line in Figure 3. The dashed line depicts a L^{-4} dependence expected for the total mass conservation as flux tubes move radially. In the range from $L = 2.5$ to 3.4, either fit is appropriate, but significant differences occur at larger L values. The parameters derived are robust when performing a multivariant fit of equation (1) to the nine prestorm profiles. Figure 4 shows the resulting empirical model. Using this model for $L = 3.32$ produces the profile plotted as a red line in Figure 1 (bottom). The standard deviation of the equatorial densities from the nine cases is slightly less than 20%, which may represent the fluctuations of the density (rather than, we believe, the uncertainty of the method).

3.2. Depletion and Refilling During and After the Storm

[11] Figures 5, 6, and 7 show three sets of the plasmagrams and the derived density profiles (black curve) together with the model prediction (red curve) from equation (1) during the storm (Figures 5 and 6, at $L = 2.8$ and $L = 2.3$, respectively) and after the storm (Figure 7 at $L = 3.1$). During the storm, at larger L the equatorial plasma density dropped to below 1/3 of the quiet time value as shown in Figure 5, but at smaller L the

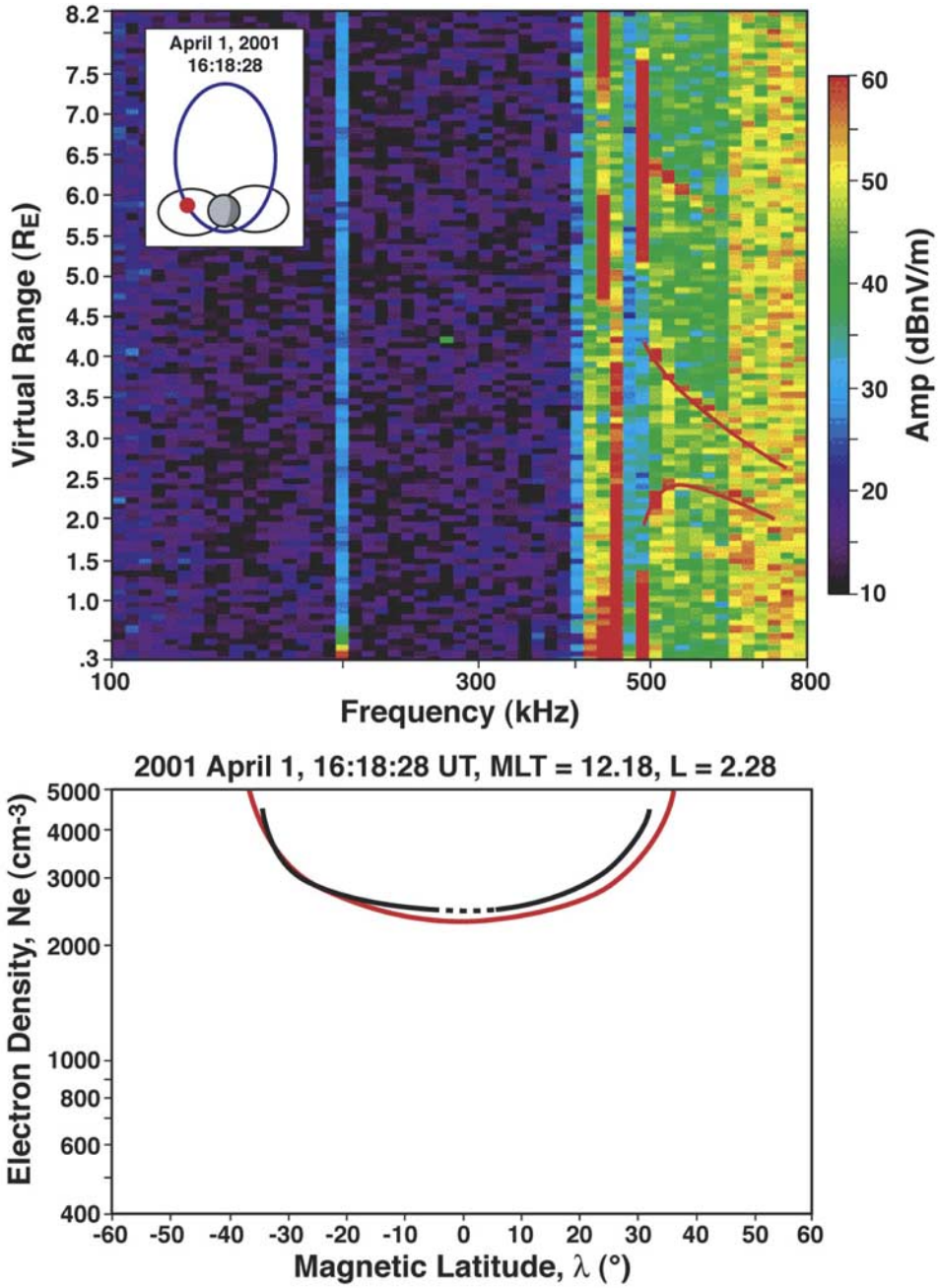

Figure 6. RPI measurements and the derived density profile during the storm event on 1 April 2001, for $L = 2.28$, in the same format as Figure 1. The electron gyrofrequency and the plasma frequency are 66.7 and 448 kHz, respectively.

plasma density is similar to the quiet time value as shown in Figure 6. After the storm, the equatorial plasma density at larger L reached the quiet time value as shown in Figure 7.

[12] To examine the time evolution of the plasma density, we define the filling ratio as the ratio of the measured equatorial density to the quiet time value at this same L value derived from equation (1). The size of the sphere in Figure 2 (bottom) is proportional to this filling ratio as shown in the legend. Depletion was observed during the storm in the region where $L > 2.2$, indicating that the plasmapause moves from $L > 3.6$ before the storm to $L \sim 2.2$ during the storm, as shown in Figure 2 (bottom) after 102 hours. Five hours after the storm onset IMAGE entered the plasmasphere and made the first measurement of two depleted flux tubes. The equatorial density dropped to less than 30% of the quiet time value during the storm, indicating that the flux tubes between the quiet time plasmapause location and the storm time one were nearly fully depleted quickly in the equatorial region.

[13] According to standard definition, although somewhat arbitrary for the convenience of statistical studies, the storm ended at 1000 UT on 2 April when *Dst* became greater than −50 nT. The start time of refilling (when the region dominated by corotation moves beyond the region of observation) cannot be defined convincingly. Nevertheless,

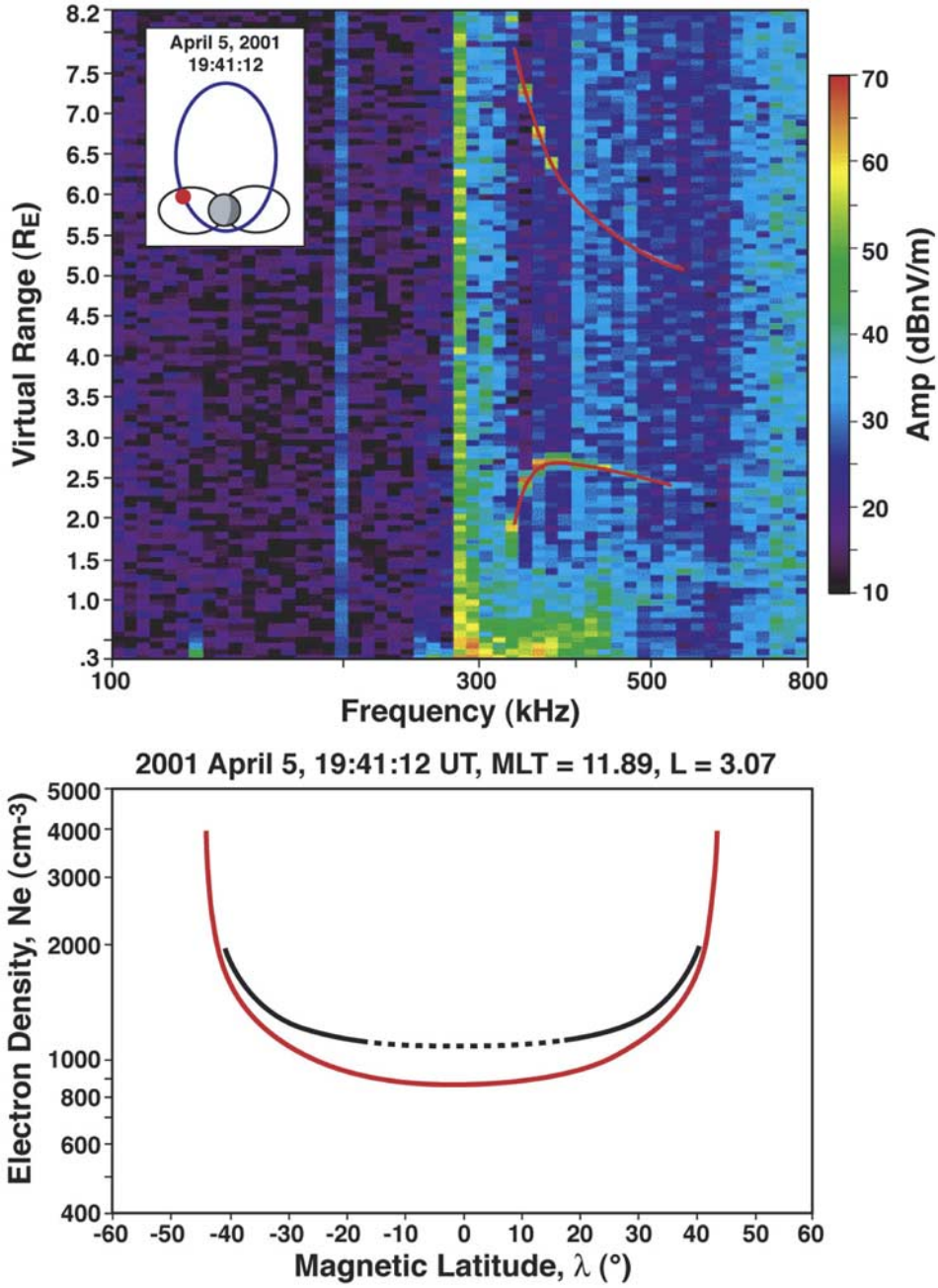

Figure 7. RPI measurements and the derived density profile after the storm event on 5 April 2001, for L = 3.07, in the same format as Figure 1. The electron gyrofrequency and the plasma frequency are 46.0 and 302 kHz, respectively.

it is clear from Figure 2 that at 0600 UT on 2 April 2001, depleted flux tubes are observed. It is quite surprising, however, that the very next observation, 14 hours later, show the plasmasphere within L = 3.6 completely filled, indicating either a refilling time of less than 14 hours, which is much quicker than some theoretical model predictions [*Rasmussen et al.*, 1993; *Tu et al.*, 2003], or that a large structure with filled flux tubes had drifted in. It is even more surprising that at the next set of measurements 14 hours later on 3 April, the flux tube at L = 2.9 appears to be depleted although the geomagnetic indices indicate no activities between the two passes. The measurements during the following pass indicate partially filled flux tubes. After 1800 UT on 4 April, the flux tubes within L = 3.7 is completely refilled at the longitudes sampled by RPI.

[14] The interpretation of the apparently filled flux tubes observed on 2 April is crucial to the global interpretation of the whole event in particular for the estimate of the refilling time. Since the RPI measurements, although based on a remote sensing technique, are restricted each to a field line, they provide only simultaneous information near local noon. Dynamic structures, on the other hand, can drift azimuthally and confuse the interpretation. To resolve the possibility, that the observed filled flux tubes are structures

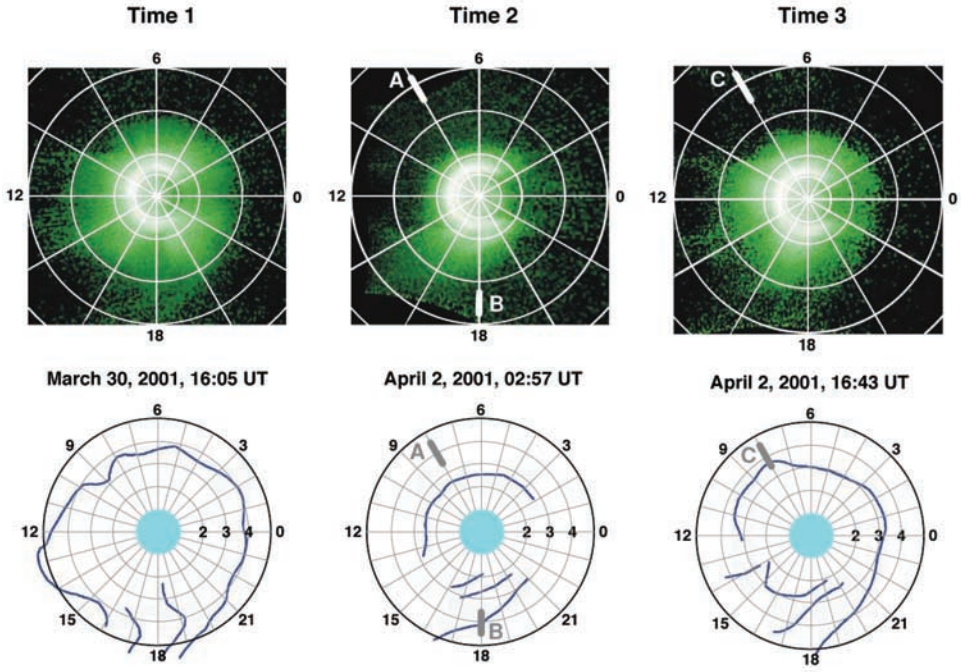

Figure 8. The EUV images taken at 1606 UT on 30 March 2001 and 0257 UT and 1645 UT on 2 April 2001. (top) Images that have been projected to the plane of the magnetic equator, in a grid of L and magnetic local time. Midnight is to the right. The smallest circle represents Earth, and the larger circles mark L values of 2, 4, and 6. (bottom) The most prominent density gradients in the images. The coordinate system is the same, but the scale has been expanded slightly for better detail. Some of the boundaries marked in Figure 8 (bottom) are difficult to distinguish in these images but are apparent when the images are displayed with other forms.

moving azimuthally, we examined the measurements from the Extreme Ultraviolet Imager (EUV) instrument on IMAGE. EUV maps the distribution of He^+ in the inner magnetosphere by imaging emissions in the He^+ resonance line at 30.4 nm [*Sandel et al.*, 2000, 2001]. Figure 8 displays several images taken during the event. Figure 8 (top) shows the images taken before the storm when the plasmasphere was in its full size (time 1), and well before (time 2), and closest to (time 3) the encounter of the filled flux tubes at 2000 UT on 2 April. Figure 8 (bottom) shows the corresponding equatorial locations of the sharpest density gradients. *Goldstein et al.* [2003] have shown that such gradients correspond to the plasmapause in steady state. Here we have marked the boundaries of high-density structures as well as the plasmapause. Figure 8 (left) shows that the plasmapause was not smooth in a range of L values from less than 4 to more than 5 before the storm (time 1). Here we should point out that as to be discussed next, because of corotation the corresponding location of the RPI measurements on the EUV images is around 0800 MLT. At that local time, the plasmapause is located near $L = 3.8$, consistent with the RPI observation of the plasmasphere up to $L = 3.8$. During the storm (time 2), the plasmapause was eroded to about $L = 2.5$, consistent with the RPI measurements during the storm, given the variability of the boundary.

[15] The EUV images help to understand from a global perspective the apparently filled flux tubes inferred from the RPI observations near 2030 UT on 2 April. The EUV image for time 2 precedes those RPI measurements made at 0630 UT and 2030 UT by about 4 and 18 hours, respectively. Thus, assuming perfect corotation, the flux tubes observed at 0630 UT and 2030 UT by RPI near noon MLT correspond to near 0800 MLT (marked "A" in Figure 8) and 1800 MLT (marked "B"), respectively, on the EUV image taken at time 2. The EUV image for time 2 shows a rather extensive drainage plume in the dusk sector, which may correspond to the flux tubes later sampled by RPI at 2030 UT. However, as shown by *Chen et al.* [1975], the drainage plume may not corotate perfectly and the drainage plume may not arrive at local noon at 2030 UT with its full strength. The image for time 3 was taken 4 hours before the RPI observation of filled flux tubes. There are a few structures on the dayside extended to $L = 6$ shown in Figure 8 (top). Also there is a bulge in the density gradient mapping extended to $L = 3.7$ near 0800 MLT ("C" in Figure 8), which may be the remnant of the drainage plume. For perfect corotation, the RPI measurements made at 2030 UT correspond to 0800 MLT on image time 3. Given such a correlation both in time and in spatial location between the drainage plume seen by EUV and the unexpected filled flux tubes observed by the RPI, we conclude that the filled flux tubes observed at local noon near 2030 UT on 2 April were most likely corotating spatial structures.

4. Discussion

[16] Our previous knowledge about the depletion and refilling processes has been limited due to the lack of

suitable observational capabilities. Most of this knowledge was based on in situ observations from International Sun-Earth Explorers (ISEE) and Dynamic Explorers (DE) satellites. The DE 1 satellite was on a high-inclination more circular orbit. The in situ data were collected at varying latitudes and/or radial distances. This makes it difficult for comparison during a dynamic process. Furthermore, the DE orbit did not cover the region near the equatorial plane at larger radial distance where the heaviest depletion may occur. The ISEE 1 satellite, on the other hand, had a highly eccentric orbit near the equatorial plane. It flew through a large range of radial distances, or L values, while remaining at similar latitude and longitude, a better orbital characteristic for plasmaspheric depletion-refilling studies. However, the orbital period of ISEE 1 was about 2 days because of its greater apogee. Measurements at the same location were made only every other day, not enough to adequately monitor the temporal variations of the depletion/refilling process. There have been reports [*Carpenter*, 1963; *Horwitz et al.*, 1984; *Carpenter and Anderson*, 1992] that the plasmapause occasionally moves much closer to the Earth and hence some plasmaspheric mass under normal conditions is lost and later refilled. These and other previous studies, using in situ observations, have had limited ability to broadly examine refilling flux tubes over a range of latitudes and L shells at any given time. As a result, it has not been directly possible to adequately test prevailing theories for the refilling process. The IMAGE orbit and the RPI remote sensing technique make it possible to quantitatively assess the depletion and refilling processes in two dimensions. A major uncertainty in the interpretation arises in the third dimension, the azimuth. The EUV images can help to resolve this uncertainty with a lower spatial and temporal resolution.

[17] The plasmapause is closely related to (but does not, except in ideal steady state, coincide with) the topological boundary in plasma flow between flux tubes that are carried from the magnetotail toward the dayside magnetopause and those that circulate continually around the Earth. The two are conveniently referred to as ''convecting'' and ''corotating,'' respectively, but it must be kept in mind that there is no discontinuity of flow velocity, the flow on either side of the boundary being the superposition of magnetospheric convection and corotation. In steady state, the topological boundary in the equatorial plane is defined by the flow line that passes through the stagnation point in the combined flow (the singular point, generally located on the dusk side, where magnetospheric convection flow is equal and opposite to corotation). Interior to the topological boundary, the ionospheric plasma source acts for a long time and is therefore able to build up a high plasma density. Exterior to the boundary, the plasma content is swept out and lost in a magnetospheric convection time (order of hours, at most), resulting in a low plasma density determined largely by the outer magnetosphere values. This explanation of the plasmapause, as a density discontinuity resulting from a topological boundary in a continuous flow, was first proposed by *Nishida* [1966] and *Brice* [1967] and is now universally accepted.

[18] To understand the changes occurring during a magnetic storm, suppose that the storm has been preceded by a long interval of quiet, so that the density within the plasmasphere has essentially reached its steady state value, and the plasmapause before the storm coincides with the flow topological boundary. During the main phase of the magnetic storm, magnetospheric convection is greatly enhanced, and the topological boundary is now located deep inside its quiet time position. The initially dense plasma between the old and the new positions is swept away toward the magnetopause (depletion of flux tubes, or erosion of the plasmasphere), and the new plasmapause coincides approximately with the new topological boundary. Our first storm-time profile observations, obtained 5 hours after the storm onset, show depleted flux tubes in the region $L > 2.2$, indicating a rather rapid depletion process and consistent with the conventional understanding. They further indicate that the new plasmapause location may be located around $L = 2.2$.

[19] During the recovery phase of the storm, magnetospheric convection weakens, and the topological boundary is now located further out (possibly near or even beyond its prestorm position). The refilling of the previously depleted flux tubes by the ionospheric source now begins. During the refilling, which may last for a relatively long time, the plasmapause does not coincide with the flow topological boundary and in fact may not be sharply defined. Although the refilling is generally believed to come from the ionospheric source, the mechanisms and detailed processes differ from model to model. As reviewed by *Singh and Horwitz* [1992], there are two classes of models. One predicts the ionospheric outflow becomes supersonic, and shocks form starting near the equator and then propagate to higher latitudes. In this scenario, higher densities should be observed near the equator. The other predicts no such shocks and hence the density is minimum near the equator. Although our observations are able to detect such profiles, they have not shown evidence for a higher density near the equator. Here we should point out that if the density does not monotonically increase from the equator toward the ionosphere, the echo traces would show signatures similar to the ones commonly observed in ground-based ionospheric sounding when waves penetrate the E layer and are reflected in the F layer [*Reinisch*, 1996]. The RPI data do not show such signatures.

[20] Observationally, the refilling rate is much more difficult to assess quantitatively. After the storm, the flow topological boundary is located in a new location, allowing more magnetospheric flux tubes to corotate and setting an environment for refilling to start. One difficulty in assessing the refilling rate observationally is that the actual location of the flow topological boundary (before the plasmasphere is filled) is difficult to determine from measurements. In other words, immediately after the flow topological boundary sets at a larger radial distance, the plasmasphere between the plasmapause and new flow topological boundary locations is essentially the same observationally until this region is substantially refilled. Namely, one is not able to determine the start of the refilling, and even less so if the location of the flow topological boundary is not steady as expected for the magnetosphere condition after a storm. Another difficulty arises because the densities of the depleted flux tubes are not near zero. Given that the magnetospheric plasma density is expected to vary significantly during a storm, one is not sure whether the residual density is a result of an already ongoing refilling process. The observed small-

scale structures on or near the plasmapause add more uncertainty to the analysis and interpretations.

[21] Since the plasmapause moved from beyond $L = 3.7$ to 2.2 during the storm, we focus our analysis around $L = 2.5 \sim 3.3$ to avoid the effects of plasmapause motion and small structures. We have shown that the filled flux tubes observed near 2030 UT on 2 April were most likely corotating structures. The start time for the refilling processes cannot be determined precisely. The three sets of RPI measurements on 3 and 4 April in Figure 2 seem to indicate a more gradual increase in the density refilling process. In less than 28 hours the flux tubes were refilled from 30% full to full from 1100 UT on 3 April to1800 UT on 4 April.

[22] Theoretical models have predicted that the refilling time is of the order of 3 days or longer [*Rasmussen et al.*, 1993; *Tu et al.*, 2003]. In particular, *Tu et al.* [2003], using the FLIP model, simulated density profiles for a quiet time case. The simulations were able to reproduce remarkably all main features in the observations from RPI. To fill from 30% full to full in the equatorial region the timescale [*Tu et al.*, 2003, Figure 4] takes about $2 \sim 3$ days, although to fill the high-latitude regions requires a much longer time. A note that we should add here is that depletion and refilling was observed by RPI at the same location but not the same flux tubes because of the plasmaspheric corotation. The simulations of the refilling start when the entire flux tubes are completely empty, but in RPI observations, even when the depletion is substantial in the equator, the high-latitude portion (higher than $\pm 45°$) of the flux tubes still contains much of the plasma. In other words, the slower refilling in simulations may be caused by the initial conditions at high latitudes used in the simulations.

5. Conclusions

[23] We have used IMAGE-RPI data to show for the first time the time evolution of the equatorial plasma density as a function of L value for a storm event in magnetic local noon. Instantaneous RPI measurements of plasma distribution along magnetic field lines from one hemisphere to the other were made in less than 2 min and the density distribution of multiple L shells is obtained in each satellite pass in less than half an hour. Such measurements were made in every orbit, about 14 hours, surrounding the large magnetic storm of 31 March 2001. From these measurements we have constructed an empirical plasmasphere density model for the quiet time before the storm specifying the density as a function of latitude and L value. This empirical model provides the means to derive the filling ratio, or the normalized equatorial density. Without such a model, the observed depletion or refilling at different L shells and/or latitudes would be difficult to assess quantitatively.

[24] For the storm event investigated the average plasmapause eroded from beyond $L = 3.7$ to $L = 2.2$ during the storm. The depletion of the magnetospheric flux tubes between $L = 2.2$ and 3.7 appeared to be rapid. Because a corotating structure, as determined from EUV images, moved azimuthally to the magnetic local noon region when an RPI measurement was made, the start time of the refilling cannot be determined precisely. Nevertheless, the plasmaspheric refilling from 30% full to full was completed in less than 28 hours (2 IMAGE orbital periods), which is substantially less than theoretical expectations.

[25] The correlation between the 2-D RPI measurements and the EUV 2-D projection images provides a powerful tool to resolve the spatial-temporal ambiguity. True 3-D observations of large-scale magnetospheric processes have become possible, although with a relatively low resolution.

[26] **Acknowledgments.** We thank I. A. Galkin and G. Khmyrov for the BinBrowser analysis support. We also thank one of the referees who made extensive detailed comments. The work at UML was supported by NASA contract NAS5-96020 under subcontract 83822 from Southwest Research Institute and by NSF under awards NSF-ATM9729775, NSF-ATM0077655, and ATM-0318643. Work at the University of Arizona was funded by a subcontract from Southwest Research Institute, under NASA contract NAS5-96020 with SwRI.

[27] Lou-Chuang Lee thanks Richard E. Denton and Robert F. Benson for their assistance in evaluating this paper.

References

Benson, R. F., V. A. Osherovich, J. Fainberg, and B. W. Reinisch (2003), Classification of IMAGE/RPI-stimulated plasma resonances for the accurate determination of magnetospheric electron density and magnetic field values, *J. Geophys. Res.*, *108*(A5), 1207, doi:10.1029/2002JA009589.

Brice, N. M. (1967), Bulk motion of the magnetosphere, *J. Geophys. Res.*, *72*, 5193.

Burch, J. L., D. G. Mitchell, B. R. Sandel, P. C. Brandt, and M. Wuest (2001a), Global dynamics of the plasmasphere and ring current during magnetic storms, *Geophys. Res. Lett.*, *28*, 1159.

Burch, J. L., et al. (2001b), Views of Earth's magnetosphere with the IMAGE satellite, *Science*, *291*, 541.

Carpenter, D. L. (1963), Whistler evidence of a 'Knee' in the magnetospheric ionization density profile, *J. Geophys. Res.*, *68*, 1675.

Carpenter, D. L., and R. R. Anderson (1992), An ISEE/whistler model of equatorial electron density in the magnetosphere, *J. Geophys. Res.*, *97*, 1097.

Carpenter, D. L., M. A. Spasojevic, T. F. Bell, U. S. Inan, B. W. Reinisch, I. A. Galkin, R. F. Benson, J. L. Green, S. F. Fung, and S. A. Boardsen (2002), Small-scale field-aligned plasmaspheric density structures inferred from the Radio Plasma Imager on IMAGE, *J. Geophys. Res.*, *107*(A9), 1258, doi:10.1029/2001JA009199.

Chen, A. J., J. M. Grebowsky, and H. A. Taylor Jr. (1975), Dynamics of mid-latitude ion trough and plasma tail, *J. Geophys. Res.*, *80*, 968.

Comfort, R. H., P. G. Richards, P. D. Craven, and M. O. Chandler (1995), Problems in simulating ion temperatures in low density flux tubes, in *Cross-Scale Coupling in Space Plasmas, Geophys. Monogr. Ser.*, vol. 93, edited by J. L. Horwitz, N. Singh, and J. L. Burch, p. 155, AGU, Washington, D. C.

Denton, R. E., M. R. Lessard, R. Anderson, E. G. Miftakhova, and J. W. Hughes (2001), Determining the mass density along magnetic field lines from toroidal eigenfrequencies: Polynomial expansion applied to CRRES data, *J. Geophys. Res.*, *106*, 29,915.

Gallagher, D. L., P. D. Craven, and R. H. Comfort (2000), Global core plasma model, *J. Geophys. Res.*, *105*, 18,819.

Goldstein, J., R. E. Denton, M. K. Hudson, E. G. Miftakhova, S. L. Young, J. D. Menietti, and D. L. Gallagher (2001), Latitudinal density dependence of magnetic field lines inferred from Polar plasma wave data, *J. Geophys. Res.*, *106*, 6195.

Goldstein, J., M. Spasojevic, P. H. Reiff, B. R. Sandel, W. T. Forrester, D. L. Gallagher, and B. W. Reinisch (2003), Identifying the plasmapause in IMAGE EUV data using IMAGE RPI in situ steep density gradients, *J. Geophys. Res.*, *108*(A4), 1147, doi:10.1029/2002JA009475.

Grebowsky, J. M. (1970), Model study of plasmapause motion, *J. Geophys Res.*, *75*, 4329.

Horwitz, J. L., R. H. Comfort, and C. R. Chappell (1984), Thermal ion composition measurements of the formation of the new outer plasmasphere and double plasmapause during storm recovery phase, *Geophys. Res. Lett.*, *11*, 701.

Horwitz, J. L., R. H. Comfort, P. G. Richards, M. O. Chandler, C. R. Chappell, P. Anderson, W. B. Hanson, and L. H. Brace (1990), Plasmasphere-ionosphere coupling: 2. Ion composition measurements at plasmaspheric and ionospheric altitudes and comparison with modeling results, *J. Geophys. Res.*, *95*, 7949.

Huang, X., and B. W. Reinisch (1982), Automatic calculation of electron density profiles from digital ionograms: 2. True height inversion of topside ionograms with the profile-fitting method, *Radio Sci.*, *17*, 837.

Huang, X., B. W. Reinisch, P. Song, J. L. Green, and D. L. Gallagher (2003), Developing an empirical density model of the plasmasphere, *Adv. Space Res.*, in press.

Newberry, I. T., R. H. Comfort, P. G. Richard, and C. R. Chappell (1989), Thermal He^+ in the plasmasphere: Comparison of observations with numerical calculations, *J. Geophys. Res.*, *94*, 15,265.

Nishida, A. (1966), Formation of a plasmapause, or magnetospheric plasma knee, by combined action of magnetospheric convection and plasma escape from the tail, *J. Geophys. Res.*, *71*, 5669.

Persoon, A. M., D. A. Gurnett, and S. D. Shawhan (1983), Polar cap electron densities from DE 1 plasma wave observations, *J. Geophys. Res.*, *88*, 10,123.

Rasmussen, C. E., S. M. Guiter, and S. G. Thomas (1993), A two-dimensional model of the plasmasphere: Refilling time constant, *Planet. Space Res.*, *41*, 35.

Reinisch, B. W. (1996), Modern ionosondes, in *Modern Ionospheric Science*, edited by H. Kohl, R. Rüster, and K. Schlegel, p. 440, Eur. Geophys. Soc., Katlenburg-Lindau, Germany.

Reinisch, B. W., G. S. Sales, D. M. Haines, S. F. Fung, and W. W. L. Taylor (1999), Radio wave active Doppler imaging of space plasma structures: Arrival angle, wave polarization, and Faraday rotation measurements with the radio plasma imager, *Radio Sci.*, *34*, 1513.

Reinisch, B. W., et al. (2000), The radio plasma imager investigation on the IMAGE spacecraft, *Space Sci. Rev.*, *91*, 319.

Reinisch, B. W., et al. (2001a), First results from the radio plasma imager in IMAGE, *Geophys. Res. Lett.*, *28*, 1167.

Reinisch, B. W., X. Huang, P. Song, G. Sales, S. F. Fung, J. L. Green, D. L. Gallagher, and V. M. Vasyliunas (2001b), Plasma density distribution along the magnetospheric field: RPI observations from IMAGE, *Geophys. Res. Lett.*, *28*, 4521.

Richards, P. G., R. W. Schunk, and J. J. Sojka (1983), Large-scale counterstreaming of H^+ and He^+ along plasmaspheric flux tubes, *J. Geophys. Res.*, *88*, 7879.

Sandel, B. R., et al. (2000), The extreme ultraviolet imager investigation for the IMAGE mission, *Space Sci. Rev.*, *91*, 197.

Sandel, B. R., R. A. King, W. T. Forrester, D. L. Gallagher, A. L. Broadfoot, and C. C. Curtis (2001), Initial results from the IMAGE extreme ultraviolet imager, *Geophys. Res. Lett.*, *28*, 1439.

Singh, N., and J. L. Horwitz (1992), Plasmaspheric refilling: Recent observations and modeling, *J. Geophys. Res.*, *97*, 1049.

Song, P., B. W. Reinisch, X. Huang, and J. L. Green (2003), Magnetospheric active wave measurements, *Adv. Space Res.*, in press.

Tsyganenko, N. A., and D. P. Stern (1996), Modeling the global magnetic field and the large-scale Birkeland current systems, *J. Geophys. Res.*, *101*, 27,187.

Tu, J., J. Horwitz, P. Song, X. Huang, B. Reinisch, and P. Richards (2003), Simulating plasmasphere field-aligned density profiles measured with IMAGE/RPI: Effects of ion heating and refilling, *J. Geophys. Res.*, *108*, 1017, doi:10.1029/2002JA009468.

D. L. Gallagher, NASA Marshal Space Flight Center, Huntsville, AL 35803, USA. (dennis.gallagher@msfc.nasa.gov)

J. L. Green and S. F. Fung, NASA Goddard Space Flight Center, MC 630, Bldg 26, Greenbelt, MD 20771-1000, USA. (green@mail630.gsfc.nasa.gov; fung@nssdca.gsfc.nasa.gov)

X. Huang, B. W. Reinisch, and P. Song, Environmental, Earth, and Atmospheric Sciences Department, Center for Atmospheric Research, University of Massachusetts Lowell, 600 Suffolk St., Lowell, MA 01854, USA. (bodo_reinisch@uml.edu; paul_song@uml.edu)

B. R. Sandel, Lunar and Planetary Laboratory, University of Arizona, 1040 East 4th Street, Room 901, Tucson, AZ 85721-0077, USA. (sandel@arizona.edu)

V. M. Vasyliunas, Max-Planck-Institut für Aeronomie, Max-Planck Str. 2, D-37191 Katlenburg-Lindau, Germany. (vasyliunas@linmpi.mpg.de)